Journal of Sound and Vibration (2001) **239**(1), 99–121
doi:10.1006/jsvi.2000.3158, available online at http://www.idealibrary.com on IDEAL®

A DISCRETE MODEL OF A VIBRATING BEAM USING A TIME-STEPPING APPROACH

S. A. Neild, P. D. McFadden and M. S. Williams

Department of Engineering Science, University of Oxford, Parks Road, Oxford, OX1 3PJ, England

(*Received* 21 *December* 1999, *and in final form* 30 *May* 2000)

A time-stepping model of a transversely vibrating, simply supported beam which allows the inclusion of non-linear damage such as a breathing crack is presented. It is based on the approximation that the mass and inertia of the beam may be lumped at points along the beam and the beam flexibility may be represented by discrete springs between rigid blocks. The advantage of a time-stepping approach over other models reported is that it enables the flexibility of the springs to be altered at any time during the analysis allowing the modelling of non-linear damage. The natural frequencies and mode shapes predicted by the model for an undamaged beam are validated against theoretical values and the representation of a non-linear mechanism in the model is compared with experimental data. The model predictions are shown to be accurate for both the undamaged and the non-linear cases.

1. INTRODUCTION

There has been interest for many years in the vibrational behaviour of cracked beams in the condition monitoring field. Numerous models of beams with cracks have been developed. These generally include either a crack that is permanently open or a "breathing" crack which opens and closes during vibration.

Many models represent the cracked beam as a series of undamaged beam finite elements with the crack represented as either a reduced stiffness in one element or a massless rotational spring at the joint between two of the beam elements. Rizos *et al.* [1] modelled a beam with an open crack as two undamaged beams connected by a spring. They used the general form of the modal shapes of the two undamaged beams along with the boundary conditions at the crack location to develop equations for the displacements on either side of the crack. The spring compliance was found using the strain energy function of the crack (reference [2]). A similar approach was used by Narkis [3] to relate the natural frequency of a beam with a double-edged crack to the crack position and depth. The method was extended to a beam with a series of cracks by Shifrin and Ruotolo [4] and to a crack in a beam with variable cross-section by Nandwana and Maiti [5]. A variation on this approach was suggested by Fernández-Sáez *et al.* [6], who calculated the displaced shapes by adding a polynomial function in terms of distance away from the crack to the undamaged displaced shapes on either side of the crack. The coefficients in the polynomials were calculated by using the boundary conditions and slope discontinuity (caused by the spring representing damage) at the crack position. Chaudhari and Maiti [7] derived equations for the mode shape of a tapered beam on either side of a crack and went on to demonstrate how the crack location and size might be calculated from the first three natural frequencies.

0022-460X/01/010099 + 23 $35.00/0

An alternative method was proposed by Mahmoud *et al.* [8]. They divided the beam along its length into many elements and, after lumping the mass for each element at the centre of the element, derived a matrix equation relating the forces and displacements of one end of an element to the other. The open crack was included as a reduced stiffness of one of the elements. A root searching technique was then used to find the natural frequencies by using the matrix equations and boundary conditions.

For most applications, applying a simple stiffness reduction is unrealistic, since most cracks open and close during oscillations, unless a static load is also applied. Gudmundson [9] noted that although the model he proposed, based on a spring representing a permanently open crack, was a good representation of the behaviour of a cantilever beam with a notch cut out, it over-predicted the change in frequency when considering a fatigue crack. Ballo [10] modelled a cracked rotating shaft with the breathing crack represented by a rotational spring element which had different properties depending on whether the curvature was positive or negative. Cheng *et al.* [11] also modelled the breathing crack as a non-linear spring, but their model was limited to the fundamental mode as they had to assume that the changes in the spring properties occur at the fundamental frequency to enable the equation of motion for the beam to be solved.

Sundermeyer and Weaver [12] demonstrated a potential use of the non-linear behaviour of a breathing crack in detecting the existence of the crack. They used a model with a bilinear spring representing the crack to show that, in theory, for a beam that is excited at two frequencies simultaneously the steady state signal consists not only of the two driving frequencies, as expected, but also a component at a frequency equal to the difference between the two driving frequencies. This was thought to be due to the bilinear stiffness properties of the spring. They concluded that this additional frequency component could be a useful indicator of bilinear behaviour resulting from damage.

Qian *et al.* [13] used a beam finite element formulation, in which different EI values for positive and negative curvature were used to represent the crack opening and closure. Rotational inertia and shear effects were not included in the formulation though the approach could be modified to include these terms (see the book by Petyt [14]). The crack mechanism assumed is very simple, since it assumes complete opening and closure always occur at zero curvature. A more general approach would allow the stiffness change to occur at some non-zero curvature, but this would be considerably more complex to implement.

The idea of representing a crack as a spring is extended here. Rather than using a rotational spring for damage and Timoshenko or Euler–Bernoulli beams between cracks, it is proposed in this paper to represent the bending and shear deformation also by using springs. The beam is divided into short rigid blocks joined with rotational and transverse springs which represent bending and shear deformation respectively. Any stiffness reduction due to a crack is represented by adjusting the rotational spring stiffness at that spring position. It is then possible to derive equations for the displacement and rotation of each rigid block in terms of the accelerations (both transverse and rotational) of the blocks and use these equations in a time-stepping method to find the response of the beam to a set of initial conditions. The advantage of this approach is that, as well as being capable of including rotational inertia and shear deformation, the spring stiffness equation at the crack position may be easily altered between time steps, allowing a bilinear breathing crack or a more complex fatigue crack to be modelled.

Firstly, the model for a simply supported beam with shear distortion ignored is derived. The natural frequencies predicted by using the model for a varying number of blocks are compared with the theoretical frequencies based on the differential equation of motion for the beam. Then the model is extended to include shear distortion and the predicted natural

frequencies are compared with the theoretical values. The model's accuracy in predicting the natural frequencies is also compared with a numerical solution for a simply supported truncated conical beam [15]. Finally, a cantilever beam version of the model including damping (represented as dash-pots at each spring position) is used to predict the dynamic response of a beam with a stiffness non-linearity and the results are compared with a simple experiment.

2. A DISCRETE APPROXIMATION TO THE BEAM

The model of the beam is based on the ideal of representing the bending and shear stiffnesses in discrete form. The beam is represented as a series of rigid blocks connected by rotational and transverse springs. The rotational spring approximates the bending of the beam and the transverse spring approximates the shear.

Firstly, the mass and inertia of the beam are approximated in lumped form. The beam is split into N blocks, those at either end being half the length of the other blocks as shown in Figure 1(a). The mass and rotational moment of inertia of each are then lumped at its centre as shown in Figure 1(b). For blocks of rectangular cross-section the mass and rotational inertia of block n are given by

$$m_n = \rho bhl_n, \quad J_n = (m_n/12)(h^2 + l_n^2), \tag{1, 2}$$

where b is the width of the beam, h is the depth and l_n is the length of the block, which is given by $L/(N-1)$ where L is the total beam length, except for the two end blocks which have length $L/2(N-1)$.

Secondly, the light flexible elements between the lumped masses and inertias are approximated by rigid elements connected by rotational and transverse springs. For the end elements, the compliance due to the half-length element in contact with the support and half of the next element is lumped at the block boundary between the end and the second element, as shown in Figure 1(c). The notation for the spring positions and the rigid blocks is defined in Figure 1(c). The displacement and rotation of the rigid block n are defined in Figure 2, where the forces acting on the block due to the springs at either end are also shown. It should be noted that as there are no springs at the supports and as the beam is simply supported, the moments at the supports (M_1 and M_{N+1}) are zero.

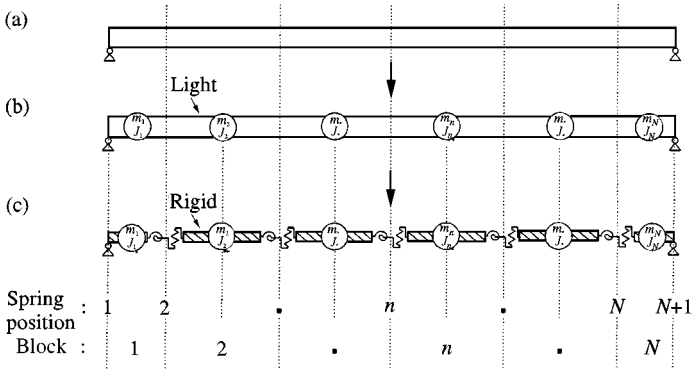

Figure 1. Modelling of the beam as discrete blocks.

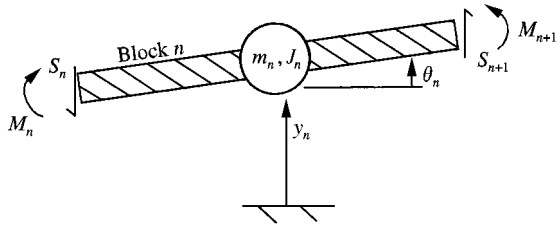

Figure 2. Forces and displacements at block n.

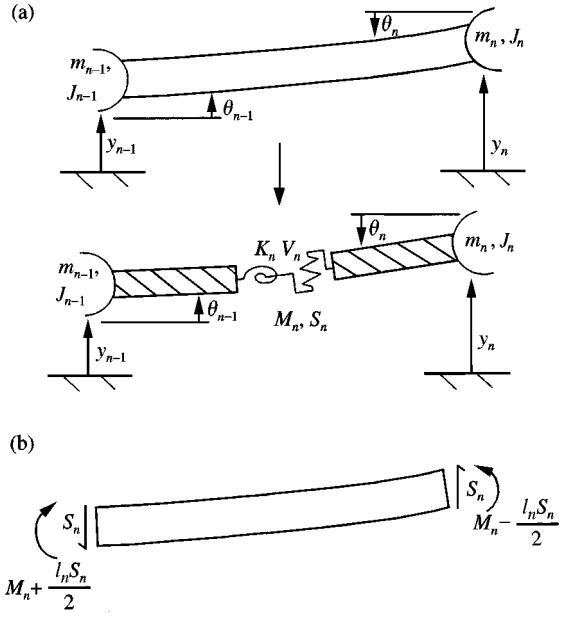

Figure 3. Spring at position n.

It is now necessary to calculate the required rotational and transverse spring stiffnesses at spring position n (K_n and V_n respectively) to model the bending and shear distortion. In the lumped model, the springs at position n are subjected to moment M_n and shear force S_n, representing the bending and shear distortion over a length l from the centre of block $n-1$ to the centre of block n, as shown in Figure 3(a) (with the exception of the end springs which represent the distortions from the support to the block position 2 or $N-1$, which is still length l). Now consider the intermediate stage where the mass and inertia have been lumped but the compliance is distributed, as in Figure 1(b). The only forces and moments on the beam element are applied at the ends. If the moment and shear at the centre of the beam element take values M_n and S_n, then the end moments are shown in Figure 3(b). The relative end rotation of this beam is given by

$$\theta_n - \theta_{n-1} = \frac{1}{EI}\left(\left(M_n + \frac{l}{2}S_n\right)l - \frac{l^2}{2}S_n\right) = \frac{l}{EI}M_n, \tag{3}$$

where I is the second moment of area for the element and E is Young's modulus. The relative end deflection (including shear distortion) is given by

$$y_n - y_{n-1} = l\theta_{n-1} + \frac{l^2}{2EI}\left(M_n + \frac{l}{2}S_n\right) - \frac{l^3}{6EI}S_n + \frac{l}{kAG}S_n$$

$$= l\theta_{n-1} + \frac{l^2}{2EI}M_n + \left(\frac{l}{kAG} + \frac{l^3}{12EI}\right)S_n, \tag{4}$$

where kA is the effective shear area and G is the shear modulus. These equations may be compared to the relative rotation and deflection equations for the beam with the lumped compliance,

$$\theta_n - \theta_{n-1} = \frac{M_n}{K_n}, \quad y_n - y_{n-1} = l\theta_{n-1} + \frac{l}{2}\frac{M_n}{K_n} + \frac{S_n}{V_n}, \tag{5, 6}$$

to give the spring stiffnesses:

$$K_n = \frac{EI}{l}, \quad V_n = \frac{kAG}{l}\frac{1}{1 + kAGl^2/12EI}. \tag{7, 8}$$

Shear distortion has only a minor effect on the vibration of a beam. Later it will be shown that for a stocky rectangular beam the effect on the frequency of the third mode is about 8% and far less for the first and second modes. It is a common assumption that shear distortion can be ignored, as for example in the Euler–Bernoulli approximation to a beam. If a rectangular cross-section beam is considered, upon taking $E/kG = 3$ (a typical value quoted by Clough and Penzien [16]), and noting that $(N-1)l = L$ where L is the total length of the beam, the transverse spring constant may be written as

$$V_n = \frac{kAG}{l}\frac{1}{1 + 1/3\lambda^2(N-1)^2}, \tag{9}$$

where $\lambda = h/L$, the depth-to-length ratio for the whole beam. It can be seen that the contribution to the transverse spring stiffness due to bending is small compared to that made by the shear distortion, which in turn has only a small effect on the overall behaviour of the beam. As the effect decreases with increasing numbers of blocks, it was decided to ignore the contribution of the bending distortion to the transverse spring, giving

$$V_n = kAG/l. \tag{10}$$

2.1. MODEL IGNORING SHEAR EFFECTS

A discrete model of a beam ignoring shear distortion is derived below. Shear distortion does affect the natural frequencies of a beam and so is included in the model in the next section; however it is worth deriving the model excluding shear distortion first as it is significantly easier. Ignoring shear distortion allows the spring representation of the deflection to be reduced to simply a rotational spring at each location and so it is possible to express the displacements purely in terms of the rotations.

2.1.1. *Derivation of the model*

The forces acting on block n are shown in Figure 2, where M_n is the moment due to deflection of the spring at position n, l_n is the length of block n, m_n is its mass and J_n is its moment of inertia. It follows that the equations of motion of the block are

$$J_n\ddot{\theta}_n = M_{n+1} - M_n + (l_n/2)(S_{n+1} + S_n), \tag{11}$$

$$m_n\ddot{y}_n = S_{n+1} - S_n. \tag{12}$$

The moment at position n can be expressed in terms of block rotations and spring stiffness,

$$M_n = K_n(\theta_n - \theta_{n-1}), \tag{13}$$

except for M_1 and M_{N+1} at either end of the beam, where the moments are zero as the beam is simply supported. If the beam is damaged this relationship between block rotation and resulting spring moments can be altered easily. For example, the spring stiffness K_n could be altered at each time step. An expression for displacement y_n may be written in terms of rotations and the displacement y_{n-1} and by differentiating twice with respect to time the rotational and linear accelerations may also be related:

$$y_n = y_{n-1} + \frac{l_{n-1}}{2}\theta_{n-1} + \frac{l_n}{2}\theta_n, \quad \ddot{y}_n = \ddot{y}_{n-1} + \frac{l_{n-1}}{2}\ddot{\theta}_{n-1} + \frac{l_n}{2}\ddot{\theta}_n. \tag{14, 15}$$

The final equation to be derived is the boundary condition that the displacement of one end with respect to the other end of the beam is zero. This may be expressed as

$$\sum_{n=1}^{N} l_n\theta_n = 0. \tag{16}$$

From these equations it is possible to express the rotational accelerations in terms of the rotations of each block and so, by using a time-stepping method, to solve the equations for given initial conditions. First, the equations must be written in matrix form. The derivation shown here is for the case where there are four blocks in the model. This is an unrealistically small number, but the derivation for larger numbers of blocks is identical.

The linear equations of motion for all the blocks may be expressed in matrix form. Since there are $N + 1$ shear forces but only N equations relating shear forces to accelerations $\ddot{y}_n$, it is only possible to eliminate N of the shear forces by using the vertical equations of motion and so the shear force S_1 is kept out of the shear vector and included as a separate vector:

$$\begin{pmatrix} m_1 & 0 & 0 & 0 \\ 0 & m_2 & 0 & 0 \\ 0 & 0 & m_3 & 0 \\ 0 & 0 & 0 & m_4 \end{pmatrix} \begin{pmatrix} \ddot{y}_1 \\ \ddot{y}_2 \\ \ddot{y}_3 \\ \ddot{y}_4 \end{pmatrix} = \begin{pmatrix} 1 & 0 & 0 & 0 \\ -1 & 1 & 0 & 0 \\ 0 & -1 & 1 & 0 \\ 0 & 0 & -1 & 1 \end{pmatrix} \begin{pmatrix} S_2 \\ S_3 \\ S_4 \\ S_5 \end{pmatrix} - \begin{pmatrix} 1 \\ 0 \\ 0 \\ 0 \end{pmatrix} S_1, \tag{17}$$

$$\mathbf{m}\{\ddot{y}\} = \mathbf{A}\{S\} - \{a\}S_1. \tag{18}$$

Similarly, the rotational equations of motion may be expressed in matrix form as

$$\begin{pmatrix} J_1 & 0 & 0 & 0 \\ 0 & J_2 & 0 & 0 \\ 0 & 0 & J_3 & 0 \\ 0 & 0 & 0 & J_4 \end{pmatrix} \begin{pmatrix} \ddot{\theta}_1 \\ \ddot{\theta}_2 \\ \ddot{\theta}_3 \\ \ddot{\theta}_4 \end{pmatrix} = \begin{pmatrix} 1 & 0 & 0 \\ -1 & 1 & 0 \\ 0 & -1 & 1 \\ 0 & 0 & -1 \end{pmatrix} \begin{pmatrix} M_2 \\ M_3 \\ M_4 \end{pmatrix}$$

$$+ \frac{1}{2} \begin{pmatrix} l_1 & 0 & 0 & 0 \\ 0 & l_2 & 0 & 0 \\ 0 & 0 & l_3 & 0 \\ 0 & 0 & 0 & l_4 \end{pmatrix} \left[\begin{pmatrix} 1 & 0 & 0 & 0 \\ 1 & 1 & 0 & 0 \\ 0 & 1 & 1 & 0 \\ 0 & 0 & 1 & 1 \end{pmatrix} \begin{pmatrix} S_2 \\ S_3 \\ S_4 \\ S_5 \end{pmatrix} + \begin{pmatrix} 1 \\ 0 \\ 0 \\ 0 \end{pmatrix} S_1 \right], \quad (19)$$

$$\mathbf{J}\{\ddot{\theta}\} = \mathbf{C}\{M\} + \tfrac{1}{2}\mathbf{L}(\mathbf{B}\{S\} + \{a\}S_1). \quad (20)$$

The $N-1$ rotational spring equations may be expressed as

$$\begin{pmatrix} M_2 \\ M_3 \\ M_4 \end{pmatrix} = \begin{pmatrix} K_2 & 0 & 0 \\ 0 & K_3 & 0 \\ 0 & 0 & K_4 \end{pmatrix} \begin{pmatrix} -1 & 1 & 0 & 0 \\ 0 & -1 & 1 & 0 \\ 0 & 0 & -1 & 1 \end{pmatrix} \begin{pmatrix} \theta_1 \\ \theta_2 \\ \theta_3 \\ \theta_4 \end{pmatrix}, \quad (21)$$

$$\{M\} = \mathbf{KD}\{\theta\}. \quad (22)$$

The compatibility equations may be written in matrix form as

$$\begin{pmatrix} 1 & 0 & 0 & 0 \\ -1 & 1 & 0 & 0 \\ 0 & -1 & 1 & 0 \\ 0 & 0 & -1 & 1 \end{pmatrix} \begin{pmatrix} y_1 \\ y_2 \\ y_3 \\ y_4 \end{pmatrix} = \frac{1}{2} \begin{pmatrix} 1 & 0 & 0 & 0 \\ 1 & 1 & 0 & 0 \\ 0 & 1 & 1 & 0 \\ 0 & 0 & 1 & 1 \end{pmatrix} \begin{pmatrix} l_1 & 0 & 0 & 0 \\ 0 & l_2 & 0 & 0 \\ 0 & 0 & l_3 & 0 \\ 0 & 0 & 0 & l_4 \end{pmatrix} \begin{pmatrix} \theta_1 \\ \theta_2 \\ \theta_3 \\ \theta_4 \end{pmatrix}, \quad (23)$$

$$\mathbf{A}\{y\} = \tfrac{1}{2}\mathbf{BL}\{\theta\}. \quad (24)$$

Finally, the boundary condition equation is

$$(l_1 \;\; l_2 \;\; l_3 \;\; l_4) \begin{pmatrix} \theta_1 \\ \theta_2 \\ \theta_3 \\ \theta_4 \end{pmatrix} = 0, \quad \{l\}^{\mathrm{T}}\{\theta\} = 0, \quad (25, 26)$$

where $\{l\}^{\mathrm{T}}$ is the transpose of $\{l\}$.

These matrix equations may be rearranged to enable the calculation of the rotational accelerations for a given set of rotations, and so may be used in a time-stepping method. Firstly, equations (22) and (18) may be used to eliminate $\{M\}$ and $\{S\}$ in equation (20). Then the $\{\ddot{y}\}$ vector may be eliminated by using equation (24) differentiated twice with respect to time. The resulting equation is

$$(\mathbf{J} - \tfrac{1}{4}\mathbf{LBA}^{-1}\mathbf{mA}^{-1}\mathbf{BL})\{\ddot{\theta}\} = \mathbf{CKD}\{\theta\} + \tfrac{1}{2}\mathbf{L}(\{a\} + \mathbf{BA}^{-1}\{a\})S_1. \quad (27)$$

This is simplified by defining $\mathbf{E}^{-1} = \mathbf{J} - \frac{1}{4}\mathbf{LBA}^{-1}\mathbf{mA}^{-1}\mathbf{BL}$ and noting that $\frac{1}{2}\mathbf{L}(\{a\} + \mathbf{BA}^{-1}\{a\})$ is the same as a column vector $\{l\}$ of the lengths of each block, giving

$$\{\ddot{\theta}\} = \mathbf{ECKD}\{\theta\} + \mathbf{E}\{l\}S_1. \tag{28}$$

This equation along with the boundary condition equations may be used to find the rotational accelerations in terms of the rotations in two steps.

Step 1: Calculate the shear force S_1 from the rotations, using the boundary condition, equation (26), differentiated twice with respect to time, and equation (28):

$$\{l\}^{\mathrm{T}}\{\ddot{\theta}\} = \{l\}^{\mathrm{T}}\mathbf{ECKD}\{\theta\} + \{l\}^{\mathrm{T}}\mathbf{E}\{l\}S_1 = 0. \tag{29}$$

Step 2: Calculate the rotational accelerations by substituting the shear force S_1, calculated in step 1, into equation (28) above.

2.1.2. *Checking the validity of the model*

In the case of an undamaged beam of uniform cross-section, it is possible to solve the continuous equation of motion of the beam to find the natural frequencies and so check the validity of the discrete model. The continuous equation of motion is [16, 17]

$$EI\frac{\mathrm{d}^4y}{\mathrm{d}x^4} + \bar{m}\frac{\mathrm{d}^2y}{\mathrm{d}t^2} - \bar{m}r^2\frac{\mathrm{d}^4y}{\mathrm{d}t^2\mathrm{d}x^2} - \frac{E\bar{m}r^2}{kG}\frac{\mathrm{d}^4y}{\mathrm{d}t^2\mathrm{d}x^2} + \frac{\bar{m}^2r^2}{kAG}\frac{\mathrm{d}^4y}{\mathrm{d}t^4} = 0, \tag{30}$$

where kA is the effective shear area of a cross-section, $\bar{m}$ is the mass per unit length and r is the radius of gyration, i.e., $r^2 = I/A$, where I is the second moment of area. The first two terms in the equation are the terms found in the elementary case where neither rotational inertia nor shear distortion are taken into account, the third term is due to rotational inertia, the fourth due to shear distortions and the last term due to a combination of rotational inertia and shear distortion. Therefore, ignoring shear effects reduces the left-hand side of the equation to the first three terms only. Weaver *et al.* [18] stated that for a simply supported beam, with or without the inclusion of rotational inertia and shear distortion, the deformed shape will take the form

$$y = \sum_{i=1}^{\infty} \sin\left(\frac{i\pi x}{L}\right)(A_i\cos(\omega_i t) + B_i\sin(\omega_i t)), \tag{31}$$

where i is the mode number $1, 2, 3, \ldots$, and ω_i is the natural frequency of mode i. Therefore, the natural frequency of mode i, upon ignoring shear distortion, ω_{ai}, may be expressed as

$$\omega_{ai} = \omega_{oi}/\sqrt{1 + (i\pi r/L)^2}, \tag{32}$$

where ω_{oi} is the natural frequency of the elementary case upon ignoring both the rotational inertia and the shear distortions:

$$\omega_{oi} = i^2\pi^2\sqrt{EI/\bar{m}L^4}. \tag{33}$$

The discrete model can now be tested. The choice of time step was checked by running the model a second time at half the time step and comparing the time signal. The time step used was in the order of 1×10^{-5} s, the precise value depending on the number of blocks in the

model. The natural frequencies predicted by the model can be calculated by using the discrete Fourier transform of the displacement signal and these can be compared to the theoretical values. Figure 4 shows the first three natural frequencies predicted by the model when using varying numbers of blocks for a rectangular cross-section beam with a depth-to-length ratio of 0·21. The frequency values are normalized by using the theoretical frequencies calculated from equations (32) and (33). It shows that the model performs very well even with a reasonably small number of blocks for the first two modes, and if 20 or more blocks are used there is less than 0·5% error in predicting the frequencies of the first three modes.

Figure 5 shows the corresponding mode shapes calculated from the time signal generated by the model when 20 blocks are used, plotted as points at each block centre, compared

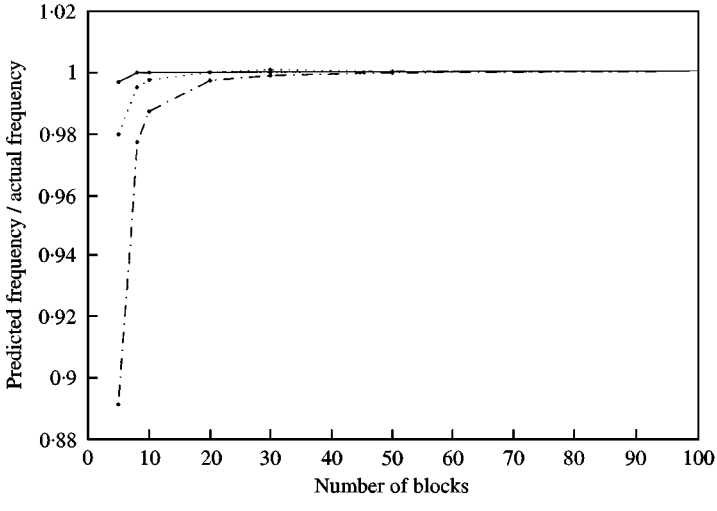

Figure 4. Frequencies predicted by the model which excludes shear deformation for varying numbers of blocks (the frequencies are normalized by using ω_{ai}, the theoretical frequency of mode i ignoring shear deformation). —●—, fundamental; ···●···, mode 2; – ● –, mode 3.

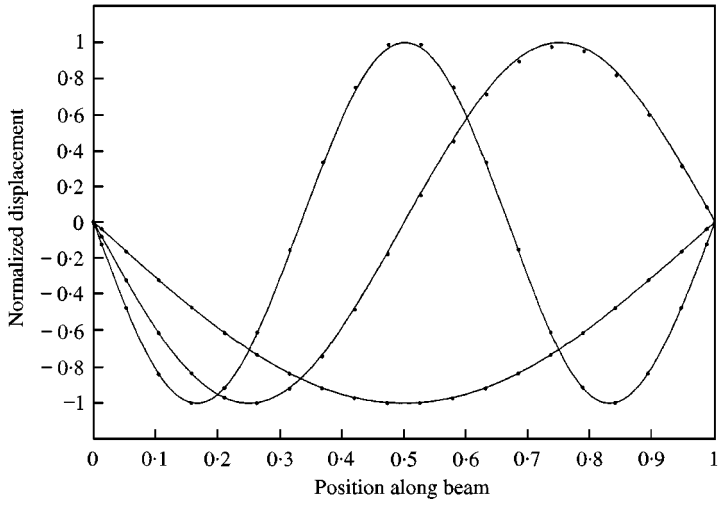

Figure 5. Mode shapes calculated using the model which excludes shear deformation. ●, calculated; ——, actual.

with the expected sinusoidal mode shapes. There is very good agreement here too between the calculated model values and the actual values for the first three modes.

2.2. MODEL INCLUDING SHEAR DISTORTION

2.2.1. Effect of shear distortion on natural frequencies

In reality a beam will be subjected to both bending and shear deflections. Although these additional shear effects make only a relatively small difference in the natural frequencies, they should not be ignored because the changes in natural frequency due to damage are also expected to be small. The effect of the shear distortions on the natural frequencies may be examined by looking again at the equation of motion of a beam, equation (30). If the expected mode shape equation (equation (31)) is substituted into the equation of motion, an equation for the natural frequencies can be found in two stages.

Firstly, if the last term on the left-hand side of the equation of motion (the term due to a combination of shear and inertial effects) is ignored, an equation for the resulting natural frequency may be derived by using the mode shape equation

$$\omega_{bi} = \frac{\omega_{oi}}{\sqrt{1 + (r\pi i/L)^2(1 + E/kG)}}, \tag{34}$$

where ω_{bi} is the natural frequency of mode i if only the term due to the combination of shear and inertial effects is ignored.

Now the effect of the last term can be examined. If a correction term κ_i, for mode i, is defined to relate ω_{bi} to the actual natural frequency ω_{ci} (which includes all the terms in equation (30)),

$$\omega_{ci}^2 = (1 + \kappa_i)\omega_{bi}^2, \tag{35}$$

then by substituting the mode shape into the equation of motion it can be shown that

$$\kappa_i = \frac{1}{2\alpha_i^2} - 1 - \frac{1}{2\alpha_i^2}\sqrt{1 - 4\alpha_i^2}, \tag{36}$$

where α_i is defined as

$$\alpha_i^2 = \frac{\bar{m}r^2}{kAG}\frac{\omega_{bi}^4}{\omega_{oi}^2} = \frac{(\pi ir/L)^4\, E/kG}{(1 + (\pi ir/L)^2(1 + E/kG))^2}. \tag{37}$$

Except when the slenderness is very low or a high mode number is being considered, α_i is small and so the expression for κ_i may be simplified to

$$\kappa_i = \alpha_i^2(1 + 2\alpha_i^2). \tag{38}$$

Table 1 shows the natural frequencies including shear deformation (ω_{ci}) and excluding shear deformation (ω_{ai}) non-dimensionalized using ω_{oi} (the natural frequency if both shear distortions and rotational inertia are ignored), for a range of values of r/L. For a rectangular section of uniform material properties the depth-to-length ratio $h/L = \sqrt{12}(r/L)$. A value of $E/kG = 3$ was used as suggested by Clough and Penzien [16] as a typical value for a rectangular cross-section.

TABLE 1

Normalized natural frequencies with and without shear distortions, where ω_a is ignoring shear deformation, ω_c is including shear deformation and ω_o is ignoring shear deformation and inertia

	ω_a/ω_o			ω_c/ω_o		
r/l	Mode 1	Mode 2	Mode 3	Mode 1	Mode 2	Mode 3
0·005	1·000	1·000	0·999	1·000	0·998	0·996
0·010	1·000	0·998	0·996	0·998	0·992	0·983
0·015	0·999	0·996	0·990	0·996	0·983	0·963
0·020	0·998	0·992	0·983	0·992	0·970	0·937
0·025	0·997	0·988	0·973	0·988	0·955	0·907
0·030	0·996	0·983	0·962	0·983	0·937	0·875
0·035	0·994	0·977	0·950	0·977	0·918	0·842
0·040	0·992	0·970	0·936	0·970	0·897	0·809
0·045	0·990	0·962	0·921	0·963	0·875	0·776
0·050	0·988	0·954	0·905	0·995	0·853	0·744
0·055	0·985	0·945	0·888	0·946	0·831	0·713

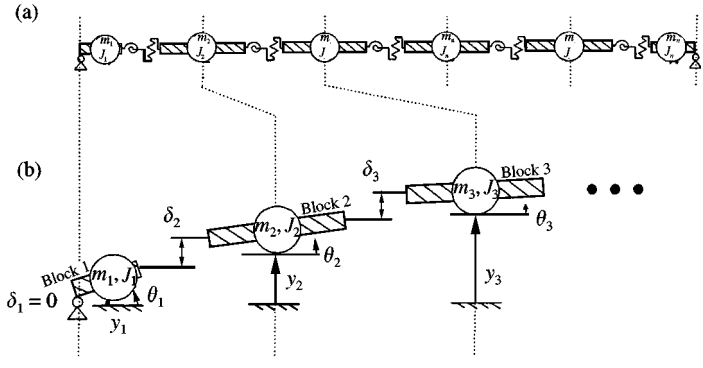

Figure 6. Diagrammatic representation of the model which includes shear deformation.

This shows that the shear effects are significant. For example, if $r/L = 0{\cdot}04$ the error in the predicted frequency of mode three is 16%. Therefore, to represent the actual beam accurately the shear distortions must be included in the model.

2.2.2. *Derivation of the model*

The major advantage in ignoring shear deformation in the previous section is that the deflections y_n of the centre of block n can be expressed as a function of the rotations of each block by using equation (24). Figure 6 shows the additional shear springs included in the model of a beam, which give rise to additional deflections δ_n. There are no shear springs at the supports so δ_1 and δ_{N+1} are zero.

Due to the deformation of the shear springs, it is now not possible to express the block deflections in terms of only the rotations of each block, as the δ deflection values are also needed. This means that the number of degrees of freedom has increased from N to $2N - 1$: i.e., there are now degrees of freedom δ_2 to δ_N in addition to the rotational degrees of

freedom θ_1 to θ_N. It should be noted that there is one less shear degree of freedom than rotational degree of freedom as there are N blocks with $N-1$ joints between them.

The equations of motion for block n are the same as for the model with no shear distortions (equations (11) and (12)), as is the equation using the rotational spring stiffness to give the moments from rotations as spring position n (equation (13)). There is an additional set of equations relating extension of the shear springs with shear force for each spring position:

$$S_n = V_n \delta_n, \tag{39}$$

where V_n is the stiffness of the shear spring (equation (10)). Equation (14) relating deflection to block rotations must be modified to take into account the shear deflections, and so too the equation relating accelerations (equation (15)). They become

$$y_n = y_{n-1} + \frac{l_{n-1}}{2}\theta_{n-1} + \frac{l_n}{2}\theta_n + \delta_n, \tag{40}$$

$$\ddot{y}_n = \ddot{y}_{n-1} + \frac{l_{n-1}}{2}\ddot{\theta}_{n-1} + \frac{l_n}{2}\ddot{\theta}_n + \ddot{\delta}_n. \tag{41}$$

Finally the boundary condition that one end of the beam may not move relative to the other (equation (16)) must be altered to include shear deflections:

$$\sum_{n=1}^{N} l_n \theta_n + \sum_{n=2}^{N} \delta_n = 0. \tag{42}$$

As before these equations are used in a time-stepping routine. To do this it is necessary to calculate the accelerations of the $2N+1$ degrees of freedom given the displacements of those degrees of freedom. It was chosen to take the displacements of the block centres ($y_1 \ldots y_N$) and the shear displacements ($\delta_2 \ldots \delta_N$) to be the degrees of freedom, although it would have been equally valid to use the rotations of the block centres ($\theta_1 \ldots \theta_N$) and shear displacements instead. The difficulty in using these equations to find the $\ddot{y}$ and $\ddot{\delta}$ values if values for y and δ are known is that there are both varying numbers of the different sets of equations and of different sets of unknowns, as shown in Table 2.

The easiest way to solve this problem is to express the equations in matrix form with vectors of values of unknowns 2 to N and additional vectors of the other unknowns S_1, S_{N+1}, $\ddot{\theta}_1$, $\ddot{y}_1$ and θ_1. Where there are more than $N-1$ equations in a set then the additional equations must be expressed separately. This approach ensures that all the matrices are

TABLE 2

Numbers of equations and unknowns

Type of unknown	Number	Type of equation	Number
S	$N+1$	vertical equations of motion	N
M	$N-1$	rotational equations of motion	N
$\ddot{\theta}$	N	equations for rotational springs	$N-1$
$\ddot{\delta}$	$N-1$	equations for shear springs	$N-1$
$\ddot{y}$	N	compatibility of displacements ($y = f(\theta, \delta)$)	N
θ	N	compatibility of accelerations ($\ddot{y} = f(\ddot{\theta}, \ddot{\delta})$)	N
		Boundary condition	1

invertible and so allows the equations to be manipulated easily. As with the previous model, the last step before calculating the accelerations is to eliminate a final unknown, this time the shear force S_{N+1}, using the boundary condition.

The derivation shown here is again for the case where there are only four blocks in the model. Firstly, the linear equations of motion for blocks 2 to 4 may be expressed in matrix form,

$$\begin{pmatrix} m_2 & 0 & 0 \\ 0 & m_3 & 0 \\ 0 & 0 & m_4 \end{pmatrix} \begin{pmatrix} \ddot{y}_2 \\ \ddot{y}_3 \\ \ddot{y}_4 \end{pmatrix} = \begin{pmatrix} -1 & 1 & 0 \\ 0 & -1 & 1 \\ 0 & 0 & -1 \end{pmatrix} \begin{pmatrix} S_2 \\ S_3 \\ S_4 \end{pmatrix} \begin{pmatrix} 0 \\ 0 \\ 1 \end{pmatrix} S_5, \tag{43}$$

$$\mathbf{m}'\{\ddot{y}'\} = \mathbf{A}'\{S'\} + \{a'\}S_5, \tag{44}$$

where the prime notation is used to distinguish the vectors and matrices from those used in the model excluding shear distortions, and the equation of motion for block 1 is written separately:

$$m_1\ddot{y}_1 = S_2 - S_1. \tag{45}$$

Similarly, the rotational equations of motion are expressed as

$$\begin{pmatrix} J_2 & 0 & 0 \\ 0 & J_3 & 0 \\ 0 & 0 & J_4 \end{pmatrix} \begin{pmatrix} \ddot{\theta}_2 \\ \ddot{\theta}_3 \\ \ddot{\theta}_4 \end{pmatrix} = \begin{pmatrix} -1 & 1 & 0 \\ 0 & -1 & 1 \\ 0 & 0 & -1 \end{pmatrix} \begin{pmatrix} M_2 \\ M_3 \\ M_4 \end{pmatrix} + \frac{1}{2} \begin{pmatrix} l_2 & 0 & 0 \\ 0 & l_3 & 0 \\ 0 & 0 & l_4 \end{pmatrix} \begin{pmatrix} 1 & 1 & 0 \\ 0 & 1 & 1 \\ 0 & 0 & 1 \end{pmatrix} \begin{pmatrix} S_2 \\ S_3 \\ S_4 \end{pmatrix} + \frac{l_4}{2} \begin{pmatrix} 0 \\ 0 \\ 1 \end{pmatrix} S_5, \tag{46}$$

$$\mathbf{J}'\{\ddot{\theta}'\} = \mathbf{A}'\{M'\} + \frac{1}{2}\mathbf{L}'\mathbf{B}'\{S'\} + \frac{l_4}{2}\{a'\}S_5, \tag{47}$$

and for block 1

$$J_1\ddot{\theta}_1 = M_2 + \frac{l_1}{2}(S_1 + S_2). \tag{48}$$

There are only $N-1$ rotational springs equations so they may be written as matrix equations without the need for an additional equation:

$$\begin{pmatrix} M_2 \\ M_3 \\ M_4 \end{pmatrix} = \begin{pmatrix} K_2 & 0 & 0 \\ 0 & K_3 & 0 \\ 0 & 0 & K_4 \end{pmatrix} \begin{pmatrix} 1 & 0 & 0 \\ -1 & 1 & 0 \\ 0 & -1 & 1 \end{pmatrix} \begin{pmatrix} \theta_2 \\ \theta_3 \\ \theta_4 \end{pmatrix} - K_2 \begin{pmatrix} 1 \\ 0 \\ 0 \end{pmatrix} \theta_1, \tag{49}$$

$$\{M'\} = \mathbf{K}'\mathbf{C}'\{\theta'\} - K_2\{b'\}\theta_1, \tag{50}$$

and similarly for the linear spring equations,

$$\begin{pmatrix} S_2 \\ S_3 \\ S_4 \end{pmatrix} = \begin{pmatrix} V_2 & 0 & 0 \\ 0 & V_3 & 0 \\ 0 & 0 & V_4 \end{pmatrix} \begin{pmatrix} \delta_2 \\ \delta_3 \\ \delta_4 \end{pmatrix}, \quad \{S'\} = \mathbf{V}'\{\delta'\} \tag{51, 52}$$

The compatibility equation may be written in matrix form,

$$\begin{pmatrix} 1 & 0 & 0 \\ -1 & 1 & 0 \\ 0 & -1 & 1 \end{pmatrix} \begin{pmatrix} y_2 \\ y_3 \\ y_4 \end{pmatrix} = \frac{1}{2} \begin{pmatrix} 1 & 0 & 0 \\ 1 & 1 & 0 \\ 0 & 1 & 1 \end{pmatrix} \begin{pmatrix} l_2 & 0 & 0 \\ 0 & l_3 & 0 \\ 0 & 0 & l_4 \end{pmatrix} \begin{pmatrix} \theta_2 \\ \theta_3 \\ \theta_4 \end{pmatrix} + \begin{pmatrix} \delta_2 \\ \delta_3 \\ \delta_4 \end{pmatrix} + 2 \begin{pmatrix} 1 \\ 0 \\ 0 \end{pmatrix} y_1, \quad (53)$$

$$\mathbf{C}'\{y'\} = \tfrac{1}{2}\,\mathbf{D}'\mathbf{L}'\{\theta'\} + \{\delta'\} + 2\{b'\}y_1, \quad (54)$$

with an additional equation for block 1:

$$y_1 = (l_1/2)\,\theta_1. \quad (55)$$

Finally, the boundary condition may be written as

$$l_1\theta_1 + (1\ \ 1\ \ 1) \begin{pmatrix} l_2 & 0 & 0 \\ 0 & l_3 & 0 \\ 0 & 0 & l_4 \end{pmatrix} \begin{pmatrix} \theta_2 \\ \theta_3 \\ \theta_4 \end{pmatrix} + (1\ \ 1\ \ 1) \begin{pmatrix} \delta_2 \\ \delta_3 \\ \delta_4 \end{pmatrix} = 0, \quad (56)$$

$$l_1\theta_1 + \{c'\}^{\mathrm{T}}\mathbf{L}'\{\theta'\} + \{c'\}^{\mathrm{T}}\{\delta'\} = 0. \quad (57)$$

As stated earlier, there are $2N - 1$ degrees of freedom (7 in this case): the displacements of the block centres $(y_1 \ldots y_N\}$ and the shear displacements $(\delta_2 \ldots \delta_N)$. For a time-stepping method, equations relating the accelerations of the degrees of freedom in terms of the displacements are required. The time-stepping method then predicts the displacements for the next time point. There are five steps to calculating the accelerations from the displacements:

Step 1: Calculate the rotations using the compatibility equations (54) and (55):

$$\theta_1 = 2y_1/l_1, \quad (58)$$

$$\{\theta'\} = 2\mathbf{L}'^{-1}\mathbf{D}'^{-1}(\mathbf{C}'\{y'\} - \{\delta'\} - 2\{b'\}y_1). \quad (59)$$

Step 2: Calculate the bending moments and shear forces between the blocks using equations (50) and (52). Note that the shear forces at either end of the beam, S_1 and S_{N+1} are still unknown (M_1 and M_{N+1} are both zero as the beam is simply supported).

Step 3: Calculate the accelerations for block 1 by using equations (45) and (48) and the compatibility equation (55), differentiated twice with respect to time. The shear force S_1 at the end of the beam is eliminated, giving

$$\ddot{\theta}_1 = \frac{4(M_2 + l_2S_2)}{4J_1 + m_1l_1^2}, \quad \ddot{y}_1 = \frac{l_1\ddot{\theta}_1}{2}. \quad (60, 61)$$

Step 4: Calculate the shear force at the end of the beam S_{N+1} by using equations (44) and (47) and equations (54), (55) and (57) differentiated twice with respect to time:

$$S_5 = \frac{1}{m_4l_4^2 + 4J_4}(2m_4l_4M_4 + (4J_4 - m_4l_4^2)S_4). \quad (62)$$

Step 5: Calculate the accelerations by using equations (44), (47) and (54) differentiated twice with respect to time, and the shear force S_{N+1}:

$$\{\ddot{\theta}'\} = \mathbf{J}'^{-1}(\mathbf{A}'\{M'\} + \tfrac{1}{2}\mathbf{L}'\mathbf{B}'\{S'\} + \tfrac{1}{2}l_4\{a'\}S_5), \tag{63}$$

$$\{\ddot{y}'\} = \mathbf{m}^{-1}(\mathbf{A}'\{S'\} + \{a'\}S_5), \quad \{\ddot{\delta}'\} = \mathbf{C}'\{\ddot{y}'\} - \tfrac{1}{2}\mathbf{D}'\mathbf{L}'\{\ddot{\theta}'\} - 2\{b'\}\ddot{y}_1 \tag{64, 65}$$

2.2.3. *Checking the validity of the model*

As with the model excluding shear deformation, it is possible to check the validity of the model for a range of numbers of blocks by using the continuous equation of motion and the sinusoidal expected mode shapes [18]. For a beam of rectangular cross-section with uniform material properties, a depth-to-length ratio of 0·127 and $E/kG = 3$, Figure 7 shows the variation of the predicted frequency with number of blocks. Figure 8 shows the same relationship for a beam with a depth-to-length ratio of 0·1. The figures show very good agreement between the model and the expected frequency values if more than 20 blocks are used.

For the case where the depth-to-length ratio is 0·1, the mode shapes for the first three modes were calculated. These are plotted for 8, 10 and 20 blocks in Figures 9, 10 and 11. The mode shapes are plotted in the form of the actual block positions, the centres of which are marked with dots. The vertical gaps between the ends of the blocks are due to the deformation of the shear springs. The true sinusoidal mode shapes are also plotted for comparison.

Rather than substituting an equation for the sinusoidal mode shape into the continuous equation of motion to find the natural frequencies, it is also possible to solve the equation for the natural frequencies numerically without using the mode shapes, although this is limited to linear vibrations. This has been done by Chen [15], who considered the vibration

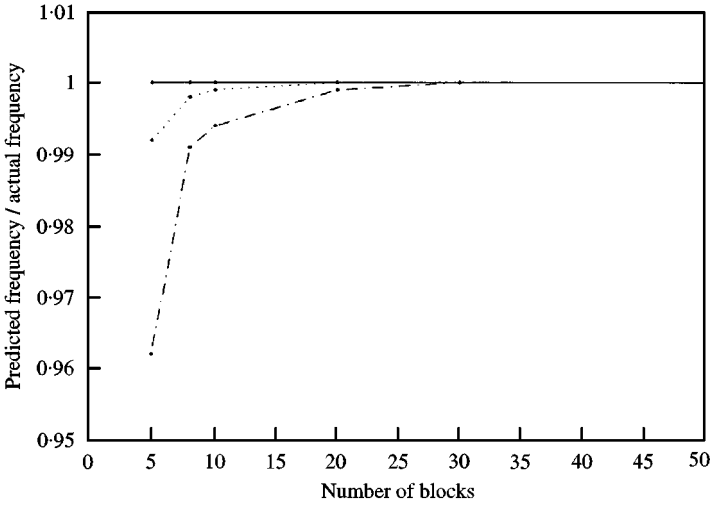

Figure 7. Frequencies predicted by the model including shear deformation for varying numbers of blocks (depth-to-length ratio = 0·127, normalized by using ω_{ci}, the natural frequency including shear deformation and rotational inertia). —●—, fundamental; ···●···, mode 2; – ● –, mode 3.

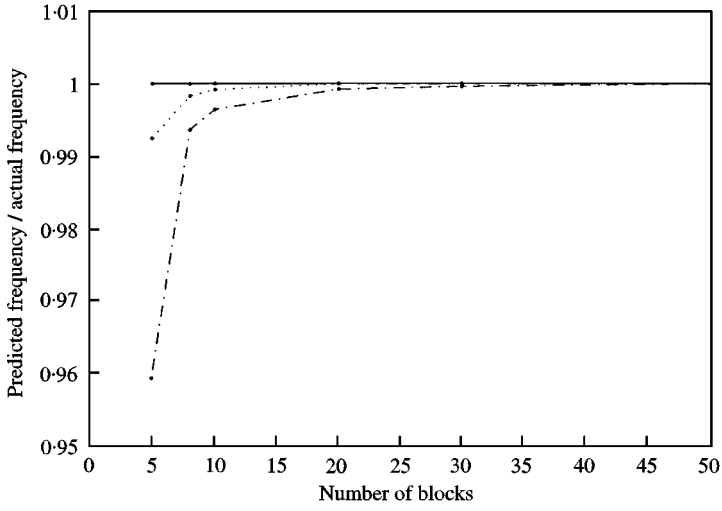

Figure 8. Frequencies predicted by the model including shear deformation for varying numbers of blocks (depth-to-length ratio = 0·1, normalized by using ω_{ci}, the natural frequency including shear deformation and rotational inertia). —●—, fundamental; ···●···, mode 2; – ● –, mode 3.

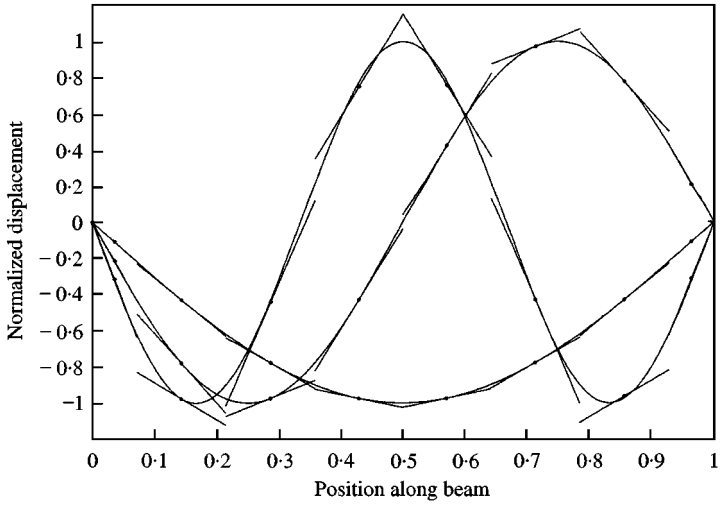

Figure 9. Mode shapes calculated by using the model including shear deformation with 8 blocks (depth-to-length ratio = 0·1). ——, actual; —●—, calculated.

of a simply supported tapered cylinder. When the taper is zero, the results from this numerical solution may be compared with the results of substituting the sinusoidal mode shape into the continuous equation of motion and to the results obtained by using the model. If the ratio of the radius of the cylinder to the length is taken to be 0·1 and the value $E/kG = 2{\cdot}93$ used by Chen is taken, then results obtained by using the numerical method agree well with the results obtained by using the sinusoidal mode shapes, confirming that the mode shape used in the substitution is the correct one. The agreement with the block model is also good, with less than 0·1% error in the prediction of the frequencies of the first five modes if 50 blocks are used, and an error of only 1·2% if 20 blocks are used.

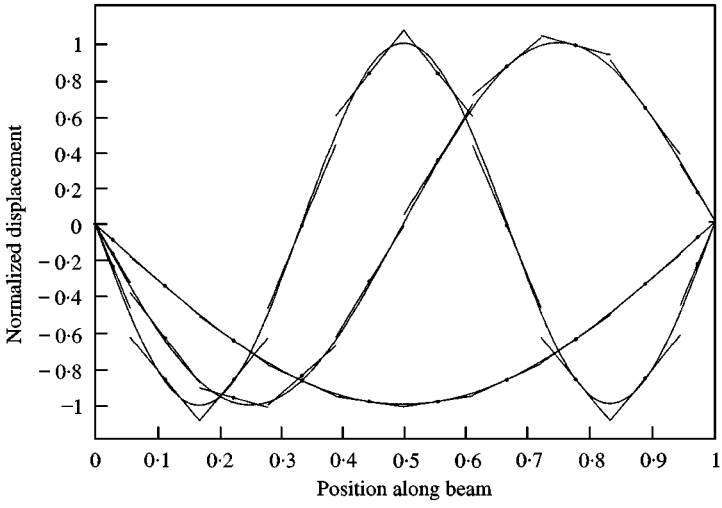

Figure 10. Mode shapes calculated by using the model including shear deformation with 10 blocks (depth-to-length ratio = 0·1). ——, actual; —●—, calculated.

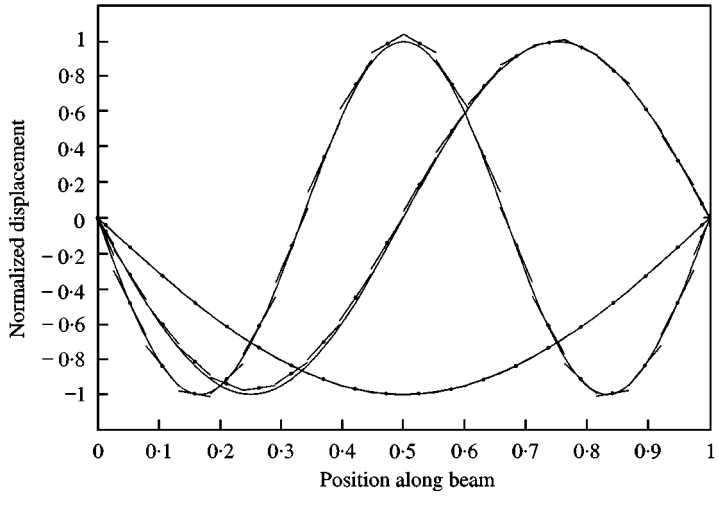

Figure 11. Mode shapes calculated by using the model including shear deformation with 20 blocks (depth-to-length ratio = 0·1). ——, actual; —●—, calculated.

For the case where the taper is non-zero, the mode shapes are not sinusoidal. If the radius of the beam at one end is twice the radius at the other end, and the ratio between the radius at the thinner end and the length of the beam is 0·1, the agreement between the numerical method and the block model is good, with the error in the first four modes being less than 0·3% with 30 blocks. Figure 12 shows the first four mode shapes calculated by using the model with 30 blocks. It should be noted that the numerical method of solving the equation of motion proposed by Chen [15] is incapable of including any non-linear damage as it requires an expression for the stiffness which is independent of time.

These tests show that the block model is an accurate predictor of the behaviour of a simply supported beam subjected to free vibration.

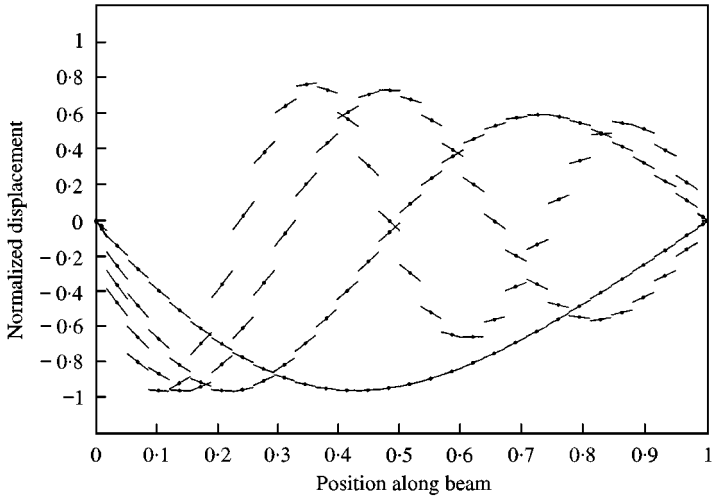

Figure 12. Mode shapes for a tapered cylindrical beam calculated by using the model including shear deformation with 30 blocks.

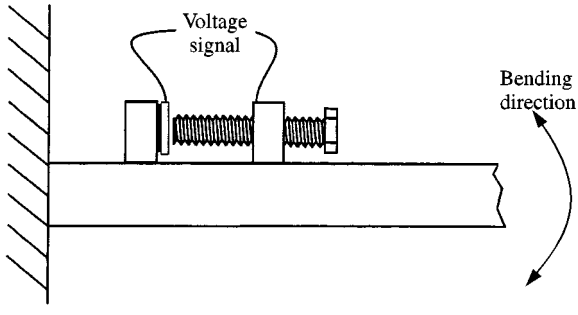

Figure 13. Stiffening beam element.

3. MODELLING NON-LINEAR DAMAGE

The model has been shown to predict to a high degree of accuracy the frequencies and mode shapes of an undamaged beam when compared to theoretical values. Now it is used to predict the behaviour of a beam with a non-linear element which is then compared with the experimental results.

3.1. EXPERIMENTAL SET-UP

One end of an aluminium bar was clamped tightly to a rigid base to form a cantilever. The bar was 25 mm wide and 6·4 mm deep, and the length of the cantilever was 0·5 m. Close to the root a non-linear section of beam was created by bonding two blocks onto the beam, with a bolt protruding out of one and almost in contact with the other (as shown in Figure 13) so that when the beam bends the blocks move closer together and the bolt comes into contact with the second block, increasing the stiffness of that region of the beam. The curvature at which contact occurs may be adjusted by using the bolt. One of the blocks was

electrically isolated from the beam so that a voltage signal could be generated indicating when contact has occurred.

The non-linear element was attached in a position which corresponded to spring position 2 in a 10 block model (the numbering system started at the root) and affected the stiffness over one block length. An accelerometer was attached to the cantilever at the mid-point of block 2. The cantilever was given an initial tip deflection of 15·5 mm and then released. The accelerometer output and the voltage across the blocks were recorded for 10 s at a sampling frequency of 8192 Hz per channel.

3.2. MODEL SET-UP

For the cantilever beam, it is necessary to adjust the model to account for the different boundary conditions. As the beam is fixed at one end, the rotation and hence displacement of the half-length block at the end are always zero since the deflection of the first beam element is represented by the rotational and shear spring positioned between the first and second rigid blocks. The boundary condition used previously is no longer true as it ensured that the relative displacement of the ends of the beam remained zero. Instead the shear force at the free end of the beam is now zero. With these new conditions the derivation of the model proceeds along much the same lines as for the simply supported beam. To model the non-linearity, the rotation of the spring at position 2 was checked at each time point and if it exceeded a threshold value $\Delta\theta_{th}$ the stiffness of the spring used for subsequent time steps was increased by a factor β, so the moment curvature equation for the spring was

$$M_2 = K_2(\beta(\theta_2 - \theta_1) - (\beta - 1)\Delta\theta_{th}), \tag{66}$$

until the rotation was found to be less than the threshold value.

In addition to the springs representing the beam compliance, damping was added at the spring positions in the form of rotational dash-pots (damping due to shear deformation was ignored as the effect of shear deformation is small for the slender beam). This was included by modifying equation (50) to

$$\{M'\} = \mathbf{K}'\mathbf{C}'\{\theta'\} - K_2\{b'\}\theta_1 + \mathbf{P}'\mathbf{C}'\{\dot{\theta}'\} - P\{b'\}\dot{\theta}_1, \tag{67}$$

where $\mathbf{P}'$ is the dash-pot coefficient P multiplied by the identity matrix.

The model beam was excited by using the theoretical statistically deformed shape (assuming no shear distortions) due to a load at the tip sufficient to deflect the tip by 15·5 mm. A 10 block model implemented in Matlab with a fourth-order Runge–Kutta routine was run for 5 s with a time increment between steps of 1×10^5 s, taking approximately 2·5 h on a 200 MHz PC with a Pentium Pro processor. The rotational inertia of the bolt assembly was ignored as the assembly was close to the root of the cantilever and the cantilever was slender so rotational inertia effects are small.

3.3. PROCESSING DATA FROM EITHER THE MODEL OR THE BEAM

Data were generated for the acceleration at position 2 and voltage signal (indicating whether the element is open or shut) for both the beam and the model. From these data three types of graph may be plotted.

Firstly, a time–frequency graph may be calculated for the first mode. This was done using the joint time–frequency distribution (see reference [19]) with the kernel suggested by Zheng and McFadden [20]. Zero padding was used to improve the frequency resolution.

Secondly, the acceleration envelope for the first mode can be calculated. This was done by applying an ideal low-pass filter to the Hilbert transform of the signal in the frequency domain and then using the inverse Fourier transform to calculate the low-frequency acceleration envelope.

Thirdly, the proportion of time the non-linear element was closed may be calculated, using the voltage signal across the blocks of the element, by setting a suitable threshold below which the blocks are in contact and the element was considered shut.

3.4. COMPARISON BETWEEN THE MODEL AND THE BEAM

Several unknowns must be established by fitting the model results to the beam results: Young's modulus, the damping coefficient, the stiffening factor β for the non-linear element and the threshold curvature $\Delta\theta_{th}$ at which the non-linear element becomes stiffer.

Initially, a linear oscillation of the beam was recorded and Young's modulus and the damping (dash-pot coefficient P) values in the model were adjusted so that the first natural frequency and the decay envelope of the acceleration of the first mode were equal in the model and the beam. Values of $E = 76{\cdot}6$ GPa and $P = 0{\cdot}046$ Nms were found to give the best fit. The effect of shear deflection is only slight so a value of $E/kG = 3$ was used. The model over-predicted the acceleration by about 3%.

A second linear test was used to set the stiffening parameter β. In this test the bolt was tightened onto the block so ensuring that for small amplitudes the mechanism remained in the closed position for the whole cycle. The stiffness of the spring nearest the root in the model was then adjusted so that the frequency of the time signal generated in the model matched the experimental frequency. β is then simply the ratio of that stiffness to the stiffness when the bolt is not in contact. The value $\beta = 2{\cdot}0$ was found to be optimal.

Then, the non-linear test was recorded (both the voltage across the non-linear element and the acceleration at block position 2). The gap between the bolt and the block was set to 0·025 mm. The threshold rotation value was set so that the initial percentage of each cycle the non-linear element was open was the same in the beam and the model. The value $\Delta\theta_{th} = 0{\cdot}004$ rad was used.

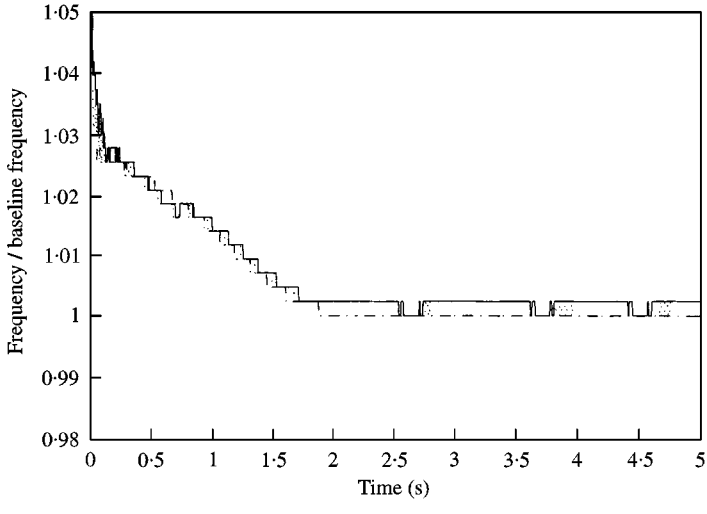

Figure 14. Time-frequency plots. ——, beam test s50/ baseline s52; ·····, beam test s51/ baseline s52; –·–·–, model test 15/ baseline frequency.

Three experimental tests were used here. Two were non-linear tests (s50 and s51) conducted under identical conditions. The third test (s52) is a linear test (the bolt in the non-linear element was retracted so the bolts never came in contact). The non-linear tests are compared to model run 15. Figure 14 shows the time–frequency plots for experimental tests s50 and s51, the frequency being normalized by using the linear test s52, and the model run 15 using the values of β and $\Delta\theta_{th}$ stated above. Linear tests where the bolt does not come in contact with the block during the oscillation are referred to as baseline tests. Figure 15 compares the acceleration envelopes for the first mode for all four tests, the experimental non-linear tests s50 and s51, the baseline linear test s52, and the model run 15. Figure 16 is a plot of the percentage of each cycle for which the element is open against the time at which that cycle occurs. The spikes in the experimental data in this figure are due to bouncing of

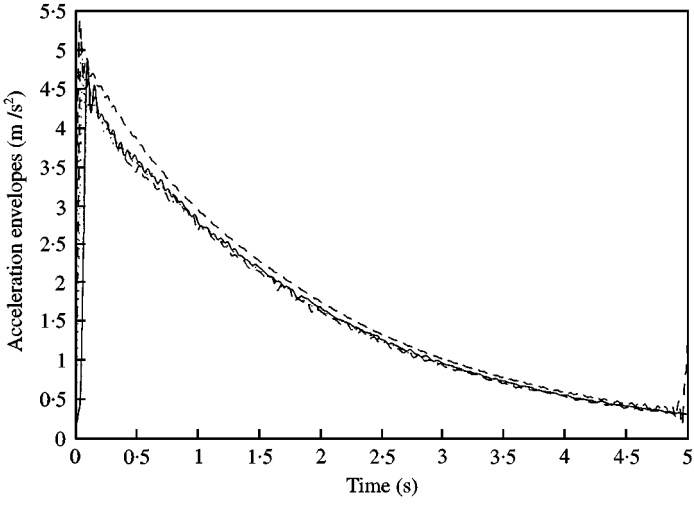

Figure 15. Fundamental mode acceleration envelopes. ——, beam test s50; ·····, beam test s51; – · – · –, baseline s52; – – –, model test 15.

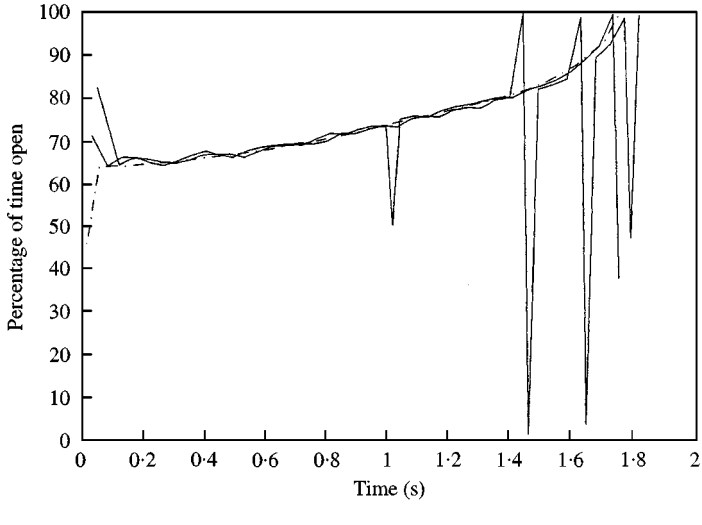

Figure 16. Plots of percentage of time open. ——, beam test s50; ——, beam test s51; – · – · –, model test 15.

the bolt against the block as the element closes. The figures show good agreement between the model and the experimental test. The agreement is expected to be very good at the beginning of Figure 16 as this was ensured when selecting the $\Delta\theta_{th}$ value. However, the model also agrees well with the experimental data for the rest of the oscillations, demonstrating its ability to model non-linear mechanisms.

4. CONCLUSION

In this paper a time-stepping model of a transversely vibrating simply supported beam has been proposed. It is based on the idea that the mass and inertia of the beam may be approximated by point masses and inertias at discrete points, and shear distortion and bending stiffness may be represented using rotational and transverse springs between rigid blocks. Two models were devised, firstly a simple one ignoring shear distortion (and hence the linear springs) and then one including the shear distortion. For the model including shear distortion, the natural frequencies and mode shapes for the first three modes, derived from acceleration data generated by using the model, compared well to theoretical values with less than a 0·1% error if 20 or more blocks were used and only a 0·6% error when a 10 block representation was used.

The advantage of this method over other methods of modelling cracked vibrating beams is that it is capable of modelling breathing cracks without the assumption that the vibration is dominated by the fundamental mode and so the crack compliance will cycle at the same frequency. Non-linear damage is modelled by altering the spring stiffness at each time step depending on the curvature of the beam at that time. The model's capabilities of predicting the non-linear behaviour have been demonstrated by using a cantilever beam with a non-linear element which resulted in a localized stiffening of the beam when the curvature exceeded a threshold value.

REFERENCES

1. P. F. RIZOS, N. ASPRAGATHOS and A. D. DIMAROGONAS 1990 *Journal of Sound and Vibration* **138**, 381–388. Identification of crack location and magnitude in a cantilever beam from the vibration modes.
2. A. D. DIMAROGONAS and S. A. PAIPETIS 1983 *Analytical Methods in Rotor Dynamics*. Amsterdam: Elsevier Applied Science.
3. Y. NARKIS 1994 *Journal of Sound and Vibration* **172**, 549–558. Identification of crack location in vibrating simply supported beams.
4. E. I. SHIFRIN and R. RUOTOLO 1999 *Journal of Sound and Vibration* **222**, 409–423. Natural frequencies of a beam with an arbitrary number of cracks.
5. B. P. NANDWANA and S. K. MAITI 1997 *Journal of Sound and Vibration* **203**, 435–446. Detection of the location and size of a crack in stepped cantilever beams based on measurements of natural frequency.
6. J. FERNÁNDEZ-SÁEZ, L. RUBIO and C. NAVARRO 1999 *Journal of Sound and Vibration* **225**, 345–352. Approximate calculation of the fundamental frequency for bending vibrations of cracked beams.
7. T. D. CHAUDHARI and S. K. MAITI 1999 *Engineering Fracture Mechanics* **63**, 425–445. Modelling of transverse vibration of beam of linearly variable depth with edge crack.
8. M. A. MAHMOUD, M. ABU ZAID and S. AL HARASHANI 1999 *Communications in Numerical Methods in Engineering* **15**, 709–715. Numerical frequency analysis of uniform beam with a transverse crack.
9. P. GUDMUNDSON 1983 *Journal of the Mechanics and Physics of Solids* **31**, 329–345. The dynamic behaviour of slender structures with cross-section cracks.
10. I. BALLO 1998 *Journal of Sound and Vibration* **217**, 321–333. Non-linear effects of vibration of a continuous transverse cracked slender shaft.

11. S. M. CHENG, X. J. WU, W. WALLACE and A. S. J. SWAMIDAS 1999 *Journal of Sound and Vibration* **225**, 201–208. Vibrational response of a beam with a breathing crack.
12. J. N. SUNDERMEYER and R. L. WEAVER 1995 *Journal of Sound and Vibration* **183**, 857–871. On crack identification and characterization in a beam by non-linear vibration analysis.
13. G.-L. QIAN, S.-N. GU and J.-S. JIANG 1990 *Journal of Sound and Vibration* **138**, 233–243. The dynamic behaviour and crack detection of a beam with a crack.
14. M. PETYT 1990 *Introduction to Finite Element Vibration Analysis*. Cambridge: Cambridge University Press.
15. R. S. CHEN 1999 *Journal of Sound and Vibration* **221**, 325–333. A novel numerical method for evaluating the natural vibration frequency of a bending bar considering rotary inertia and shear effect.
16. R. W. CLOUGH and J. PENZIEN 1975 *Dynamics of Structures*. New York: McGraw-Hill.
17. F. S. TSE, I. E. MORSE and R. T. HINKLE 1978 *Mechanical Vibrations*: *Theory and Applications*. Allyn and Bacon Inc., second edition.
18. W. WEAVER, S. TIMOSHENKO and D. H. YOUNG 1990 *Vibration Problems in Engineering*. New York: Wiley, fifth edition.
19. L. COHEN 1989 *Proceedings of the IEEE* **77**, 941–981. Time–frequency distributions — a review.
20. G. T. ZHENG and P. D. MCFADDEN 1999 *ASME Transactions Journal of Vibration and Acoustics* **121**, 328–333. A time–frequency distribution for analysis of signals with transient components and its application to vibration analysis.